Available online at www.sciencedirect.com
ScienceDirect
Continental Shelf Research 27 (2007) 1568–1583
CONTINENTAL SHELF RESEARCH
www.elsevier.com/locate/csr

An estimate of the suspended particulate matter (SPM) transport in the southern North Sea using SeaWiFS images, in situ measurements and numerical model results

Michael Fettweis*, Bouchra Nechad, Dries Van den Eynde

Management Unit of the North Sea Mathematical Models (MUMM), Royal Belgian Institute of Natural Sciences, Gulledelle 100, 1200 Brussels, Belgium

Received 10 March 2006; received in revised form 9 January 2007; accepted 17 January 2007
Available online 2 February 2007

Abstract

A study is presented where satellite images (SeaWiFS), in situ measurements (tidal cycle and snapshot) and a 2D hydrodynamic numerical model have been combined to calculate the long term SPM (Suspended Particulate Matter) transport through the Dover Strait and in the southern North Sea. The total amount of SPM supplied to the North Sea through the Dover Strait is estimated to be 31.74×10^6 t. The satellite images provide synoptic views of SPM concentration distribution but do not take away the uncertainty of SPM transport calculation. This is due to the fact that SPM concentration varies as a function of tide, wind, spring-neap tidal cycles and seasons. The short term variations (tidal, spring-neap tidal cycle) have not been found in the satellite images, however seasonal variations are clearly visible. Furthermore the SPM concentration in the satellite images is generally lower than in the in situ measurements. The representativness of SPM concentration maps derived from satellites for calculating long term transports has therefore been investigated by comparing the SPM concentration variability from the in situ measurements with those of the remote sensing data. The most important constraints of satellite images are related to the fact that satellite data is evidence of clear sky conditions, whereas in situ measurements from a vessel can be carried out also during rougher meteorological conditions and that due to the too low time resolution of the satellite images the SPM concentration peaks are often missed. It is underlined that SPM concentration measurements should be carried out during at least one tidal cycle in high turbidity areas to obtain representative values of SPM concentration.

Keywords: Cohesive sediments; Suspended particulate matter transport; Satellite imagery; SPM measurements; Hydrodynamic numerical model; Southern North Sea; Dover Strait

1. Introduction

The fine grained sediment dynamics in the southern North Sea have been the subject of many scientific and applied studies. There is clear evidence of long-term net inflow through the Dover Strait and thus also of net suspended particulate matter (SPM) transport into the North Sea (Prandle et al., 1993, 1996). Gerritsen et al. (2001) underline that this transport is the main source of recent fine-grained sediments in the North Sea. Extensive scientific literature on the residual SPM transport

*Corresponding author. Tel.: +32 2 7732132; fax: +32 2 7706972.
E-mail address: m.fettweis@mumm.ac.be (M. Fettweis).

0278-4343/$ - see front matter © 2007 Elsevier Ltd. All rights reserved.
doi:10.1016/j.csr.2007.01.017

through the Dover Strait exists; the values vary between $[2.5-57.8] \times 10^6$ t/yr (Eisma, 1981; van Alphen, 1990; Lafite et al., 1993; Velegrakis et al., 1997; McManus and Prandle, 1997). These big differences reflect partially the high temporal and spatial variability of the influx but have their origin also in the way the SPM measurements have been carried out, in the small number of SPM concentration measurements on which the calculations were based as well as the differences in the way the residual SPM transport was calculated. Accurate knowledge of the SPM flux through the Dover Strait is important in order to set up a sediment budget, to identify the sources and sinks of mud in the North Sea and to investigate the influence of anthropogenic activities, such as dredging and dumping on the local cohesive sediment transport.

The purpose of this paper is to present a study where satellite images (SeaWiFS), in situ measurements and a hydrodynamic numerical model have been combined to calculate the long term averaged SPM transport through the Dover Strait and in the southern North Sea. The use of optical remote sensing methods to produce SPM concentration maps benefits from the satellite's capabilities to view a wide area and to provide synoptic views of SPM concentration distribution. The disadvantages are mainly that the data are limited to the surface layer, that good data exist only during cloud-free daytime and that the time resolution is low. For the Belgian continental shelf about 60 (partially) cloud free images per year are available. In order to cope with the fact that only surface values are available, the method presented by Van den Eynde et al. (2006) has been applied in which in situ measurements of SPM concentrations during a tidal cycle and satellite images have been used to calculate the depth averaged SPM concentration distribution. The low time resolution prevents an accurate computation of the sediment flux when using:

$$T = \int_0^t \int_0^h u(z,t)c(z,t)\,\mathrm{d}z\,\mathrm{d}t, \qquad (1)$$

where T is the sediment flux per unit width, h is the water depth, $u(z,t)$ is the current velocity normal to the section and $c(z,t)$ the SPM concentration. Prandle et al. (1996) wrote that the SPM dynamics in tidal waters are mainly determined by water depth h, eddy diffusivity K_z and settling velocity w and that the residual transport closely approximates

$$T \approx \int_0^t \int_0^h u(z,t)\,\mathrm{d}z\,\mathrm{d}t \int_0^t \int_0^h c(z,t)\,\mathrm{d}z\,\mathrm{d}t, \qquad (2)$$

when $K_z > wh$. In coastal waters, such as the southern North Sea, with a water depth between 10–50 m and a K_z of 0.01 m^2/s the settling velocity must be <1 mm/s. This is a value in agreement with measured settling velocities of flocs and aggregates in estuaries and in the North Sea (van Leussen, 1994; Winterwerp, 1998; Mikkelsen and Pejrup, 2001). Both formulae have been used to calculate the SPM transport.

The paper is structured as follows. In Section 2 the study area is described with special emphasis on the Belgian coastal waters, followed by a presentation of the method used to obtain SPM concentration maps from satellite images and in situ measurements and of the hydrodynamic numerical model used to simulate the water flow in the area. In Section 3 the sediment transport results based on the hydrodynamic model and the satellite images using Eqs. (1) and (2) are presented. The question of the representativness of SPM concentration maps derived from satellites for calculating long term averaged transport is discussed in Section 4 by comparing the SPM concentration variability from in situ measurements with remote sensing data. Some general conclusions are offered in Section 5.

2. Methods

2.1. Study area

The study area is the southern North Sea and the Dover Strait (Fig. 1) and specifically the Belgian coastal zone. This area is especially of interest due to the occurrence of a high turbidity zone. It is characterised by depths between 5–35 m, a mean tidal range at Zeebrugge of 4.3 m (2.8 m) at spring (neap) tide and by maximum current velocities of more than 1 m/s. The winds are mainly from the southwest and the highest waves occur during north-westerly winds. The SPM concentration measurements indicate variation in the coastal zone between a minimum of 20–70 mg/l and a maximum of 100–1000 mg/l; low values (<10 mg/l) have been measured in the offshore area. Based on numerical results Fettweis and Van den Eynde (2003) conclude that the decreasing residual water transport vectors, the shallowness of the area and the difference in magnitude between neap and spring tidal currents

and their effect on the erosion and transport capacity are responsible for the occurrence of the turbidity maximum.

2.2. SPM concentration maps derived from satellite images

The SPM flux in the southern North Sea is calculated using the depth averaged SPM concentration maps derived from satellite images, which are obtained in two steps. First the images from the Sea-viewing Wide Field-of-view Sensor (SeaWiFS) (http://oceancolor.gsfc.nasa.gov/SeaWiFS) aboard the Orbview2 spacecraft have been processed. SeaWiFS measures the reflected sunlight at the Top Of Atmosphere (TOA) at 8 bands from the visible to near infrared wavelengths centred at 412, 443, 490, 510, 555, 670, 765 and 865 nm. The

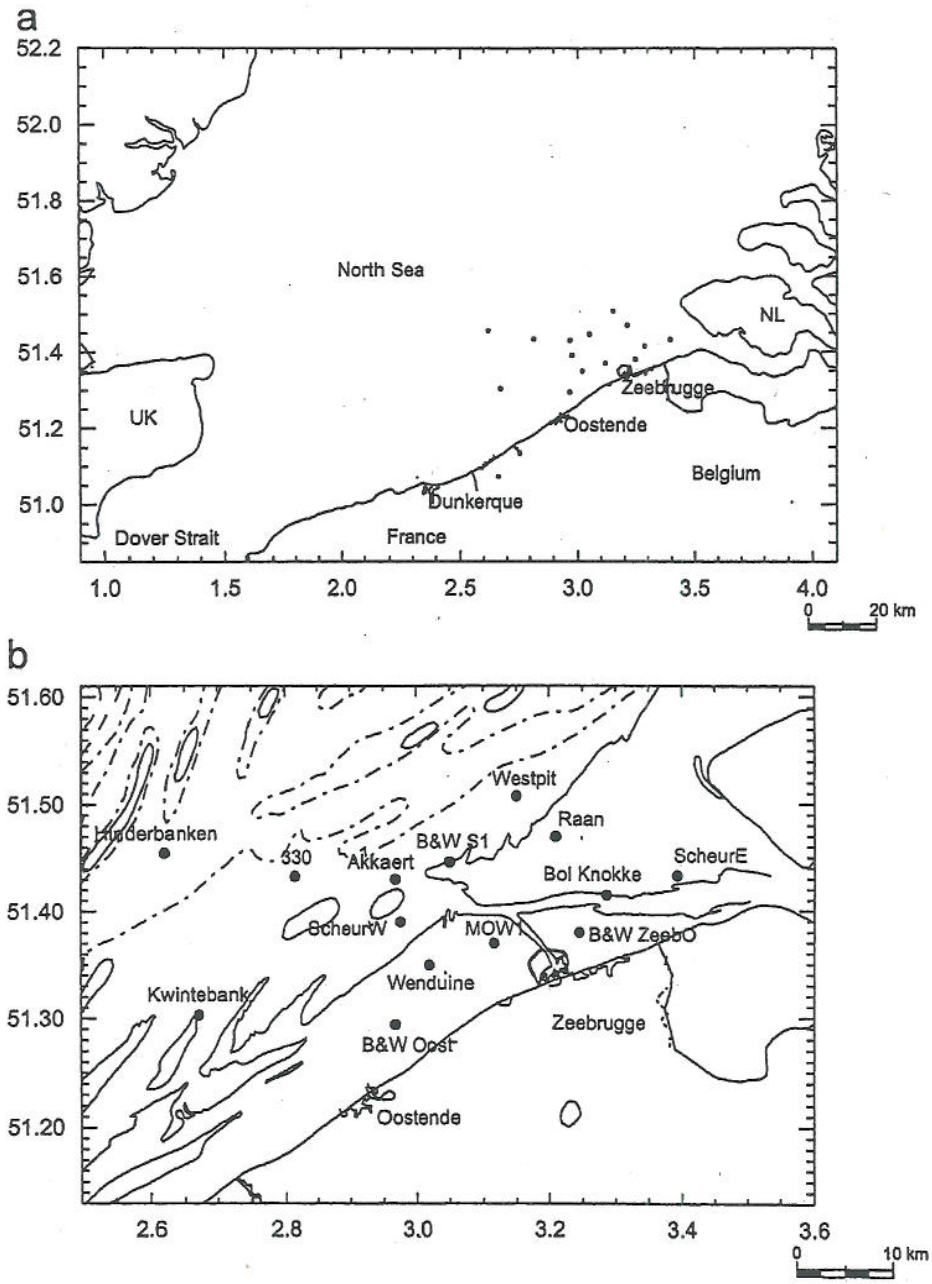

Fig. 1. (a) Map of the southern North Sea and the Dover Strait and (b) map of the Belgian coastal area (full line: 10 m, dash dot: 20 m, dash: 30 m MSL). The dots indicate the position of the tidal cycle measurement stations (Table 3). The x- and y-coordinates are in longitude (°E) and latitude (°N).

SeaDAS 4.5 software (http://oceancolor.gsfc.nasa.gov/seadas/), extended to turbid waters (Ruddick et al., 2000) is used to process these TOA radiances into atmospherically corrected reflectance by removing atmosphere contributions (scattering and absorption from air molecules, ozone and aerosols) and sea-water interface effect and finally providing the water-leaving reflectance spectrum denoted hereafter by $\rho_w^{i=412,\ldots,865\,\mathrm{nm}}$, where i refers to the i^{th} band of SeaWiFS. A bio-optical model, which has been designed for Belgian coastal waters (see Appendix A), is used to convert $\rho_w^{670\,\mathrm{nm}}$ into SPM concentration by:

$$c = 4.29 + \frac{56.68\rho_w^{670\,\mathrm{nm}}}{0.187 - \rho_w^{670\,\mathrm{nm}}}\,[\mathrm{mg/l}]. \quad (3)$$

The next step in the processing was to multiply the surface SPM concentration values by area-specific correction factors in order to obtain vertical averaged SPM concentrations, see Van den Eynde et al. (2006). These correction factors, which vary during a tidal cycle, represent the ratio between surface and depth-averaged SPM concentration and were derived from in situ tidal SPM concentration profiles taken on the Belgian continental shelf (BCS). In the Belgian coastal areas the correction factors were between 1.25 and 2.2, the maxima occurring at about 1 h before high water and around low water and are related to maximum/minimum current velocity. In the offshore area, on the other hand, the ratio between the depth-averaged and the surface SPM concentration stays nearly constant over the entire tidal cycle and is limited to values below 1.1. The SPM concentration measurements also indicate that the highest correction factor corresponds generally well with the periods of high surface SPM concentration (>50 mg/l). Because we have no information outside the BCS on timing of correction factors during a tidal cycle, it was decided to neglect the relative timing during a tidal cycle and to apply correction factors as a function of SPM concentration solely. A maximum correction factor of 2 was used for high surface concentration (>50 mg/l) and the lowest for areas with low surface SPM concentration (<20 mg/l). For SPM concentrations in between, a linear interpolation of the correction factor was used. In Fig. 3 the SPM concentration before and after correction along 51.3°N latitude is shown.

2.3. Measurements and instruments

The SPM concentration data, which are discussed here, have been collected from the R/V Belgica as snapshots or during tidal cycles. The tidal cycle measurements have been measured between March 1999 and February 2005 using a Sea-Bird SBE09 SCTD carousel sampling system (containing twelve 101 Niskin bottles), which was kept at least 4.5 m below the surface and about 3 m above the bottom. Every 20 min a Niskin bottle was closed, resulting in

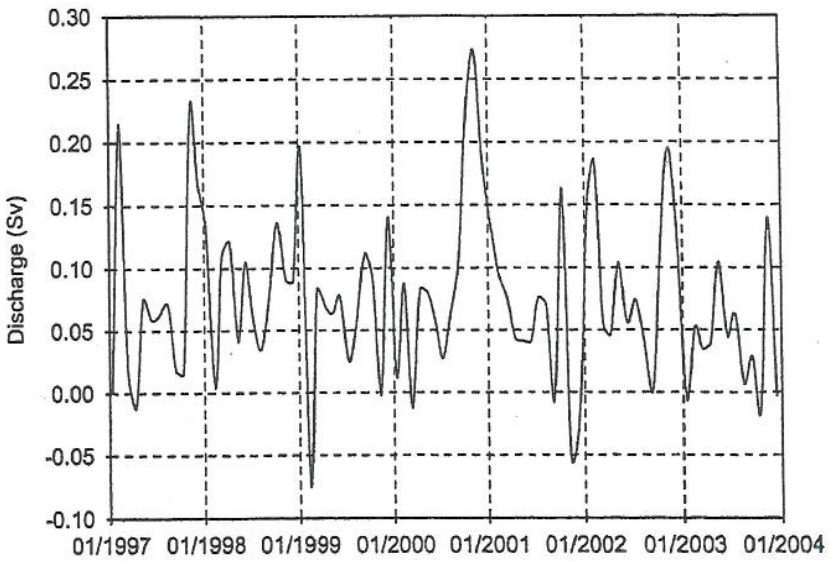

Fig. 2. Monthly averaged residual discharge through the Dover Strait (1997–2004) simulated by the 2D hydrodynamic model of the northwest European continental shelf. Positive values are towards the North Sea, negative towards the English Channel.

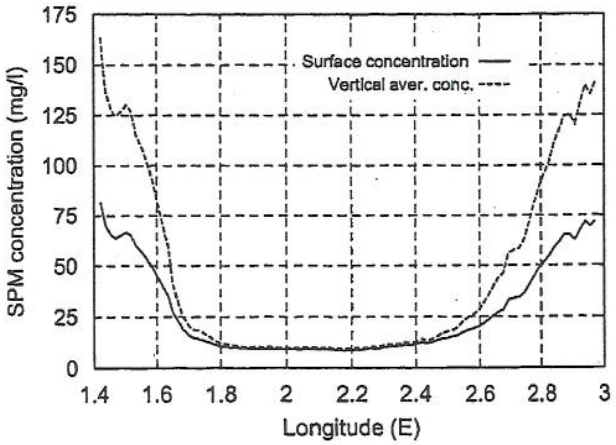

Fig. 3. Yearly averaged SPM concentration derived from 362 SeaWiFS satellite pictures of the southern North Sea along 51.3°N latitude. Comparison between surface (without correction) and vertical averaged SPM concentration (multiplied with a correction factor) is shown.

about 40 samples per tidal cycle. Every hour the carousel was taken on board of the vessel and the water samples were filtered on board using pre-weighted GF/C filters, which were later dried and weighed to obtain SPM concentration. In the framework of MUMM's Monitoring Program snapshots of SPM concentration were sampled at 3 m below surface. The procedure of sampling is similar to that described above, except that they are not made throughout the tidal cycle.

2.4. Hydrodynamic model description

The residual water transport and discharge has been modelled using the public domain 3D hydrodynamic COHERENS model (Luyten et al., 1999). This model has been developed between 1990 and 1998 in the framework of the EU-MAST projects PROFILE, NOMADS and COHERENS. The hydrodynamic model solves the momentum equation, the continuity equation and the equations of temperature and salinity. The equations of momentum and continuity are solved using the 'mode-splitting' technique. COHERENS disposes of different turbulence schemes, including the two equation k–ε turbulence model.

For the current application a 2D implementation of the COHERENS model to the northwest European continental shelf was used. The model grid has a resolution of 5′ (= 0.0833°) in longitude and 2.5′ (0.0417°) in latitude (about 5 × 5 km). Meteorological surface forcing is from the forecasts of the UK Meteorological Office at Bracknell. Four semi-diurnal tidal components (M_2, S_2, N_2, K_2) and four diurnal tidal components (O_1, K_1, P_1, Q_1) are used to force the tidal elevation on the open boundaries of the continental shelf model.

3. Results

3.1. Numerical simulation of residual discharge

The residual water transport u_{res} per water depth is calculated in every point of the grid using the following expression:

$$u_{res} = \sum_{i=1}^{n} u_i h_i \Big/ \sum_{i=1}^{n} h_i, \tag{4}$$

where u_i is the current velocity, h_i the water depth and n the number of time steps considered for averaging. The seasonally and yearly residual water transport through the Dover Strait for the period 1997–2004 are presented in Table 1 and the monthly residuals in Fig. 2. The yearly residual discharge varies between 0.041 Sv in 2003 and 0.099 Sv in 2000 (average over the whole period is 0.073 ± 0.020 Sv). The residual discharge is on average highest during autumn (0.101 Sv) and lowest during summer (0.052 Sv). Without meteorological influence the difference between the seasons would be very small (0.044–0.048 Sv) and the yearly residual discharge would be limited to 0.046 Sv. The residual discharge is determined during autumn to be about 62% by meteorological influences, whereas during summer the wind effects are limited to about 20%.

Table 1
Seasonally and yearly residual discharge (Sv) through the Dover Strait towards the North Sea for the period 1997–2004 simulated with the 2D hydrodynamic model of the northwest European shelf

	Spring	Summer	Autumn	Winter	Year
1997	0.040	0.050	0.136	0.079	0.076
1998	0.089	0.057	0.106	0.082	0.083
1999	0.070	0.065	0.077	0.067	0.070
2000	0.074	0.065	0.227	0.029	0.099
2001	0.042	0.047	0.030	0.102	0.055
2002	0.069	0.038	0.146	0.130	0.096
2003	0.063	0.033	0.040	0.027	0.041
2004	0.069	0.059	0.049	0.064	0.060
1997–2004	0.065	0.052	0.101	0.073	0.073

These values are of the same order of magnitude as the values found in literature. Prandle (1993) obtained discharge values of 0.036 Sv (only M_2 tidal constituent), 0.045 Sv (wind-forced residual) and 0.087 Sv (total) by analyzing 11 months of current data measured with HF radar between June 1990 and March 1991. Salomon et al. (1993) have calculated with a 2D tide-driven hydrodynamic model (grid resolution $3 \times 3\,km^2$) a residual discharge of 0.0374 Sv. With the measured wind at La Hague, corrected by adding 1.8 m/s from the south and averaged twice a week they simulated a yearly discharge (period 1983–1991) through the Strait of 0.114 ± 0.016 Sv. Bailly du Bois et al. (1995) estimated the water flux through the Dover Strait as 0.097 Sv up to 0.195 Sv for 1988, they based their values on the dispersal of radio nuclides. By combining HF-radar measurements with ADCP current velocity profiles Prandle et al. (1996) calculated a residual discharge of 0.094 Sv, 50% of which is due to wind effects. Garreau (1997) has simulated a residual discharge of 0.105 Sv using a yearly averaged wind velocity and direction (6 m/s, 305°).

3.2. SPM concentration in the southern North Sea

In total 362 SeaWiFS images were collected from September 1997 to April 2004. Among these images, 172 scenes are entirely cloud-free. Most of the 362 images have been affected by less than 30% of clouds which were flagged during the processing of SPM concentration maps. The images have been grouped per season and have been processed to obtain vertically averaged SPM concentration, 37% of the images are from spring, 27% from summer, 13% from autumn and 23% from winter. A map of the seasonal surface and vertically averaged SPM concentration is given in Figs. 4 and 5 respectively. The maximum surface SPM concentrations in the southern North Sea are situated between 75 and 100 mg/l during autumn and winter and 25–50 mg/l during spring and summer. The highest values are found in the Belgian–Dutch coastal zone and in the mouth of the Thames estuary. In the Dover Strait the maxima are limited to about 15 mg/l (summer) up to 50 mg/l (winter). The meteorological data from the UKMO together with information on cloud cover from the satellite imagery have been

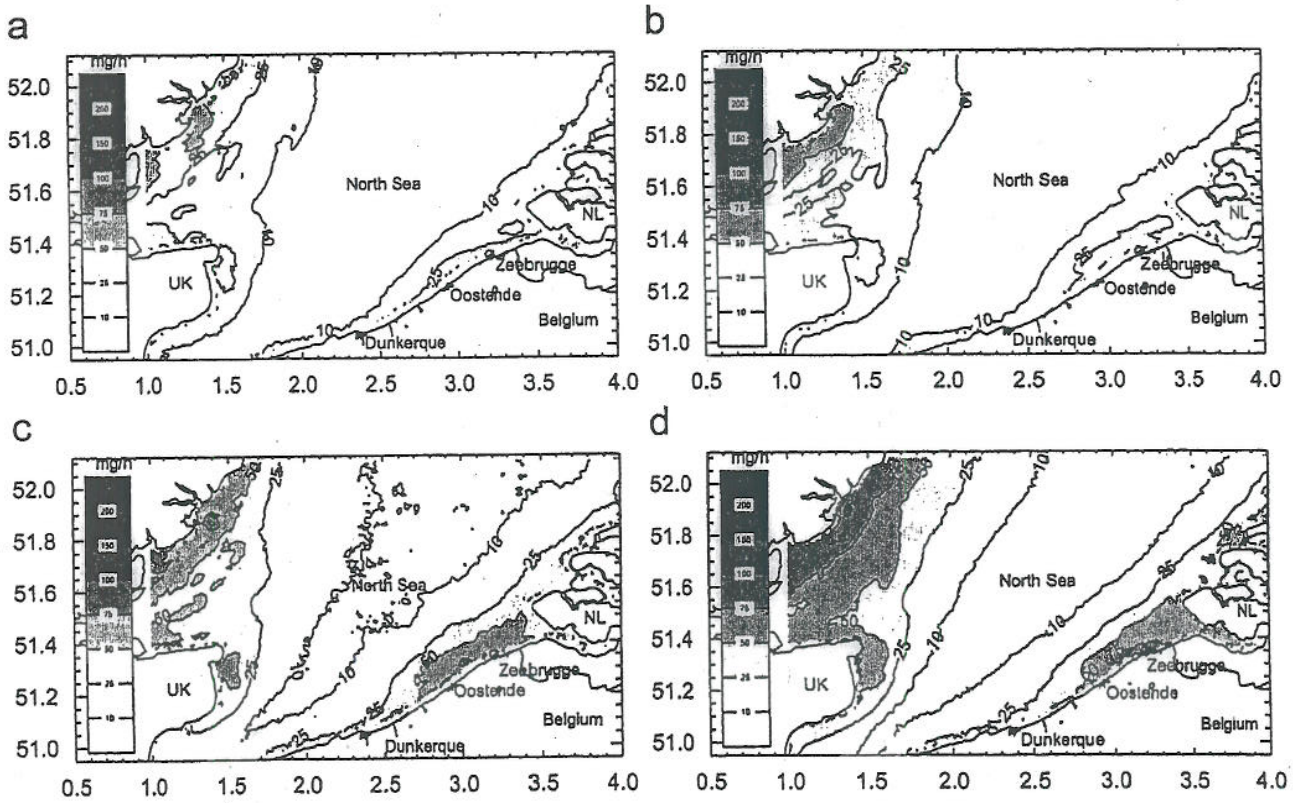

Fig. 4. Seasonal averages of SPM surface concentration in the southern North Sea derived from 362 SeaWiFS images (1997–2004). The x- and y-coordinates are in longitude (°E) and latitude (°N), respectively: (a) spring; (b) summer; (c) autumn; and (d) winter situation.

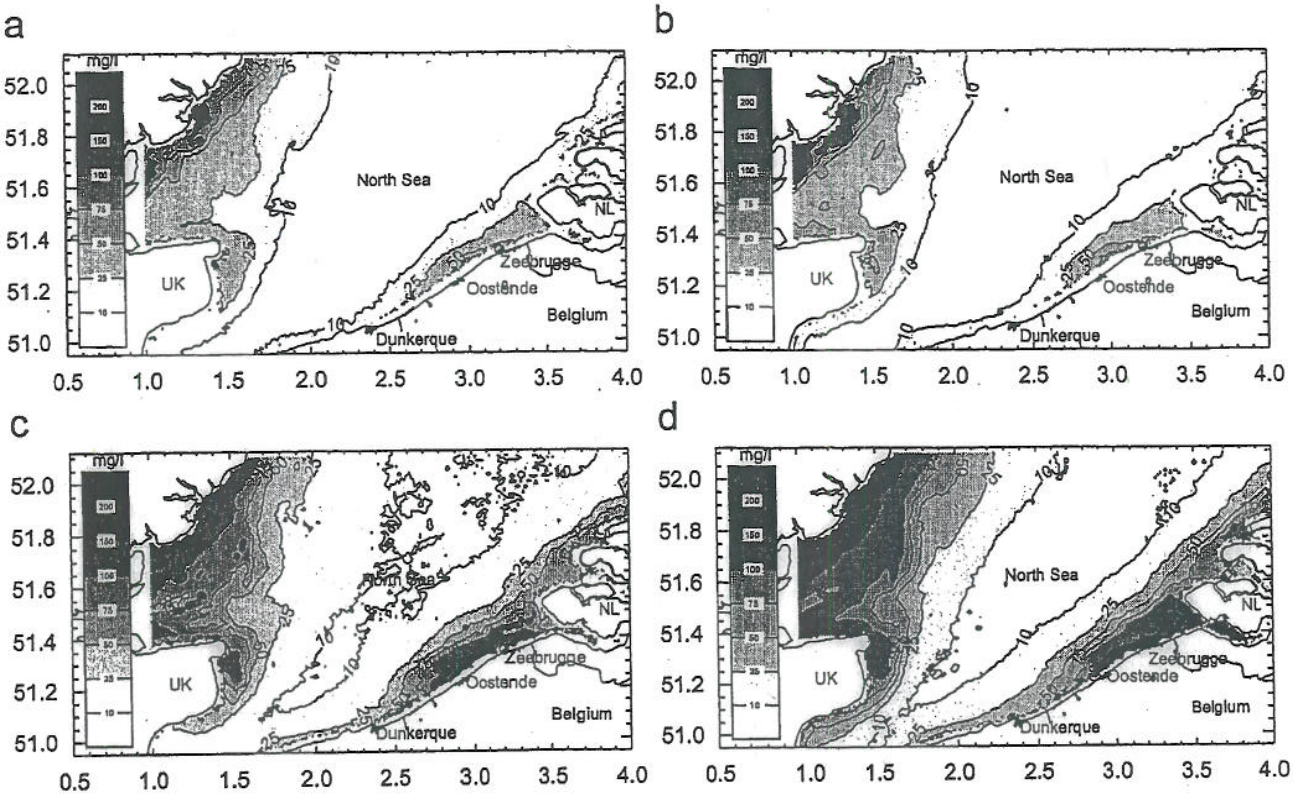

Fig. 5. Seasonal averages of vertically corrected SPM concentration (vertically averaged) in the southern North Sea derived from 362 SeaWiFS images (1997–2004). The x- and y-coordinates are in longitude (°E) and latitude (°N), respectively: (a) spring; (b) summer; (c) autumn; and (d) winter situation.

used to calculate the mean wind speed at station 330 during cloudy and cloud-free sky conditions in the satellite pictures. No clouds are present in the pixel in 83% of the images with the other 17% being cloudy. The mean wind speed during cloud-free conditions was 3.7 m/s (maximum 11.3 m/s), which is a little lower than the 4.8 m/s mean wind speed during clouded conditions.

The SPM concentration has been measured during 38 tidal cycles between March 1999 and February 2005 from the R/V Belgica, see Table 2. 14% of the measurements were made during spring, 23% during summer, 26% during autumn and 37% during winter. The mean wind speed during all measurements was 6.7 m/s. The results presented in Fig. 6 show the mean SPM concentration distribution in the different stations.

The SPM concentration has also been measured in the framework of MUMM's Monitoring Program; these data are snapshots of SPM concentration at 3 m below surface and have thus not been measured throughout the tidal cycle. The data have been extracted from the BMDC database (http://www.mumm.ac.be/datacentre) for the period 1987–2004 and in the stations where at least 10 samples exist. In total 719 samples are available from which 35% during spring, 4% during summer, 34% during autumn and 27% during winter. In Fig. 7 the mean SPM concentration distribution is shown.

3.3. SPM transport in the southern North Sea

The net sediment flux has been calculated through the Dover Strait (51.0°N) and through a cross section at 51.9°N using Eqs. (1) and (2). Eq. (1) has been applied in two ways. First the 362 SPM concentration fields derived from satellite pictures have been multiplied by the velocity field at that same moment and summed (method 1); second the velocity fields at every model time step (10 min) have been multiplied with the linearly interpolated SPM concentration at that time and also summed (method 2). For Eq. (2) the seasonally averaged velocity fields and SPM concentration maps have been used (method 3). The results, which are

Table 2
Measurements of SPM concentration in the Belgian coastal area during 38 tidal cycles (Fig. 1)

Location	cmp.	Season	Wind	Tide	SPM concentration (mg/l)			
			(m/s)		Max	Min	Avg	Stdv (%)
B&W Oostende	99/07	Win	3.84	NT	137.9	16.7	46.1	62
"	02/27	Aut	4.86	MT	55.4	16.1	29.7	35
"	03/04	Win	2.36	ST	988.7	67.2	281.1	80
"	04/16	Sum	10.48	NT	63.9	13.5	32.3	43
Wenduine	01/06	Win	6.66	MT	299.8	55.6	140.4	51
MOW1	01/06	Win	3.16	MT	303.7	27.2	120.8	61
"	02/27	Aut	7.22	NT	115.6	30.1	53.4	39
"	03/04	Win	9.13	ST	657.5	40.0	213.0	79
"	03/22	Sum	6.04	MT	105.3	17.9	47.9	45
"	04/24	Aut	5.91	ST	289.7	35.0	119.9	72
"	04/25	Aut	5.50	NT	176.5	28.4	89.4	55
"	05/02	Win	3.69	MT	559.3	30.2	163.9	74
"	05/07	Spr	5.89	NT	121.6	31.3	61.8	43
"	05/15	Sum	1.27	MT	440.5	10.1	104.2	86
B&W ZeebO	00/08	Spr	4.27	ST	552.2	42.4	214.2	79
"	00/14	Spr	9.56	NT	182.5	16.5	75.7	62
"	00/26	Aut	12.67	MT	287.2	48.5	115.2	54
Bol Knokke	00/31	Aut	10.31	MT	32.5	11.8	17.5	26
"	02/01	Win	9.31	MT	296.2	27.9	96.8	55
"	02/01	Win	15.41	ST	308.4	128.2	203.2	38
"	02/06	Win	2.81	MT	96.4	21.9	49.9	38
"	02/14	Sum	9.03	ST	47.1	7.1	22.1	50
Raan	01/01	Win	7.70	MT	212.8	35.5	104.2	45
Scheur E	01/17	Sum	3.53	MT	59.1	12.0	28.6	48
Scheur W	01/29	Aut	9.06	ST	117.6	35.2	70.2	38
"	02/06	Win	6.92	ST	69.1	14.3	31.1	38
Kwintebank	03/15	Spr	3.52	MT	7.6	2.7	4.5	26
"	03/17	Sum	5.78	NT	8.6	3.8	5.4	17
"	03/25	Aut	11.18	ST	63.0	8.3	26.6	44
"	04/04	Win	6.10	NT	28.2	10.9	15.4	25
"	04/05	Win	8.08	ST	108.2	20.6	41.3	38
"	05/15	Spr	2.87	MT	17.4	2.6	6.2	51
Hinderbanken	04/25	Aut	1.71	NT	7.2	2.1	3.4	31
330	99/17	Sum	4.60	ST	25.1	4.4	7.4	46
Akkaert	02/14	Sum	5.79	ST	11.6	5.1	7.9	22
B&W S1	00/19	Sum	12.76	NT	15.5	5.9	9.1	22
"	05/07	Spr	8.19	MT	92.0	19.0	43.9	50
Westpit	01/17	Sum	5.55	MT	20.7	6.6	9.9	28

The water samples have been taken at about 3 m above the bottom. (Cmp = campaign number, spr = spring, sum = summer, aut = autumn, win = winter, ST = spring tide, wind = mean wind speed during the measurements, MT = mean tide, NT = neap tide, max (min) = maximum (minimum) SPM concentration during the tidal cycle, avg = tidally averaged SPM concentration, stdv = relative standard deviation).

presented in Fig. 8 show clearly that differences exist between the methods. The two figures (Fig. 8b and c) are qualitatively similar in that SPM enters the southern North Sea through the Dover Strait where it bifurcates along the English and continental coastal zone and flows towards the north. Using solely the 362 satellite pictures and the corresponding velocity fields (Fig. 8a) gives a transport direction, which does not correspond with the typical long term residual circulation.

The residual SPM transport through the Dover Strait and through a cross section at 51.9°N are given for method 2 and 3 in Table 3. The value of the SPM transport is dependant on the method. Using method 2 (Eq. (1) and interpolation) the highest SPM transport occurs during autumn and

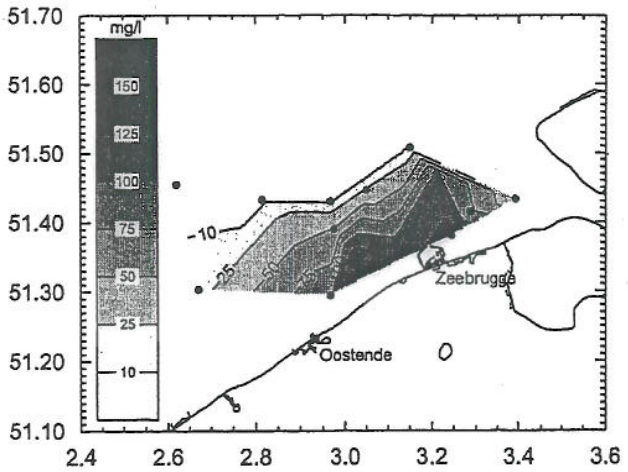

Fig. 6. Mean SPM concentration in the tidal cycle stations during the period 1999–2005. The samples have been taken at about 3 m from the bottom. The x- and y-coordinates are in longitude (°E) and latitude (°N), respectively.

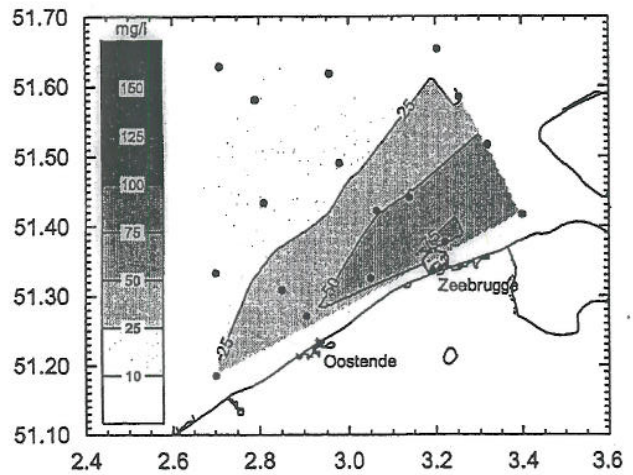

Fig. 7. Mean of SPM concentrations from 'snapshot' samples collected in MUMM's monitoring stations during the period 1987–2004. Only stations with at least 10 samples have been selected. The samples have been taken at 3 m below the surface. The x- and y-coordinates are in longitude (°E) and latitude (°N), respectively.

the lowest during summer (Dover Strait) and spring (51.9°N). Using method 3 (Eq. (2)) the highest SPM transport is calculated during autumn and the lowest during spring (Dover Strait) and summer (51.9°N), the seasonal transports are shown in Fig. 9. The SPM transport per year through the Dover Strait amounts to 31.74×10^6 t (method 3); from which about 40% flows through the English and 60% through the French part of the Strait. The results are about 60% smaller when method 2 is applied (22.26×10^6 t/yr). It can be seen that the SPM transport values are of the same order of magnitude as most of the recently published ones: $[22–30] \times 10^6$ t/yr (Eisma and Irion, 1988), 17×10^6 t/yr (Van Alphen, 1990); 19.2×10^6 t/yr (Lafite et al., 1993) and $[21.6 \pm 2.1] \times 10^6$ t/yr (Velegrakis et al., 1997). McManus and Prandle (1997) used numerical model results and in situ measurement data of SPM concentration to obtain a yearly averaged value of 44.4×10^6 t/yr. Sediment accumulation measurements in the Kattegat and the Skagerrak resulted in a four times higher accumulation rate than previously accepted (de Haas, 1997). This could imply a SPM transport through the Dover Strait of at least 46×10^6 t/yr.

4. Discussion

4.1. SPM transport

The transport through the Dover Strait and the 51.9°N section have to be more or less in equilibrium, because the major source of SPM in the southern North Sea is the Dover Strait and no significant deposition areas of mud exist in the Southern Bight (Eisma, 1981). Important local sources of SPM are the rivers (Thames, Rhine-Meuse, Scheldt), seafloor and coastal erosion and primary production. Accurate values however do not exist; the Thames supplies about 0.7×10^6 t/yr (Dyer and Moffat, 1998), the Rhine about 1.7×10^6 t/yr (Eisma, 1981) and erosion of the Holocene mud layers in front of the Belgian coast is estimated as $0–2.4 \times 10^6$ t/yr (Bastin, 1974) or about 3×10^6 t/yr (Fettweis and Van den Eynde, 2003). The total input of SPM from these sources is thus situated between 2.4×10^6 and 5.4×10^6 t/yr. The SPM input is probably higher because primary production, seafloor erosion outside the Belgian coastal area and coastal erosion are not included. The difference between inflow and outflow is 38.31×10^6 t/yr for method 2 and 9.08×10^6 t/yr for method 3. The latter is closer to the sum of the local SPM sources, which indicates that method 3 is—with the available data—the most accurate one.

4.2. Variability of SPM concentration

The satellite images provide synoptic views of SPM concentration distribution but do not take away the uncertainty of SPM transport calculation,

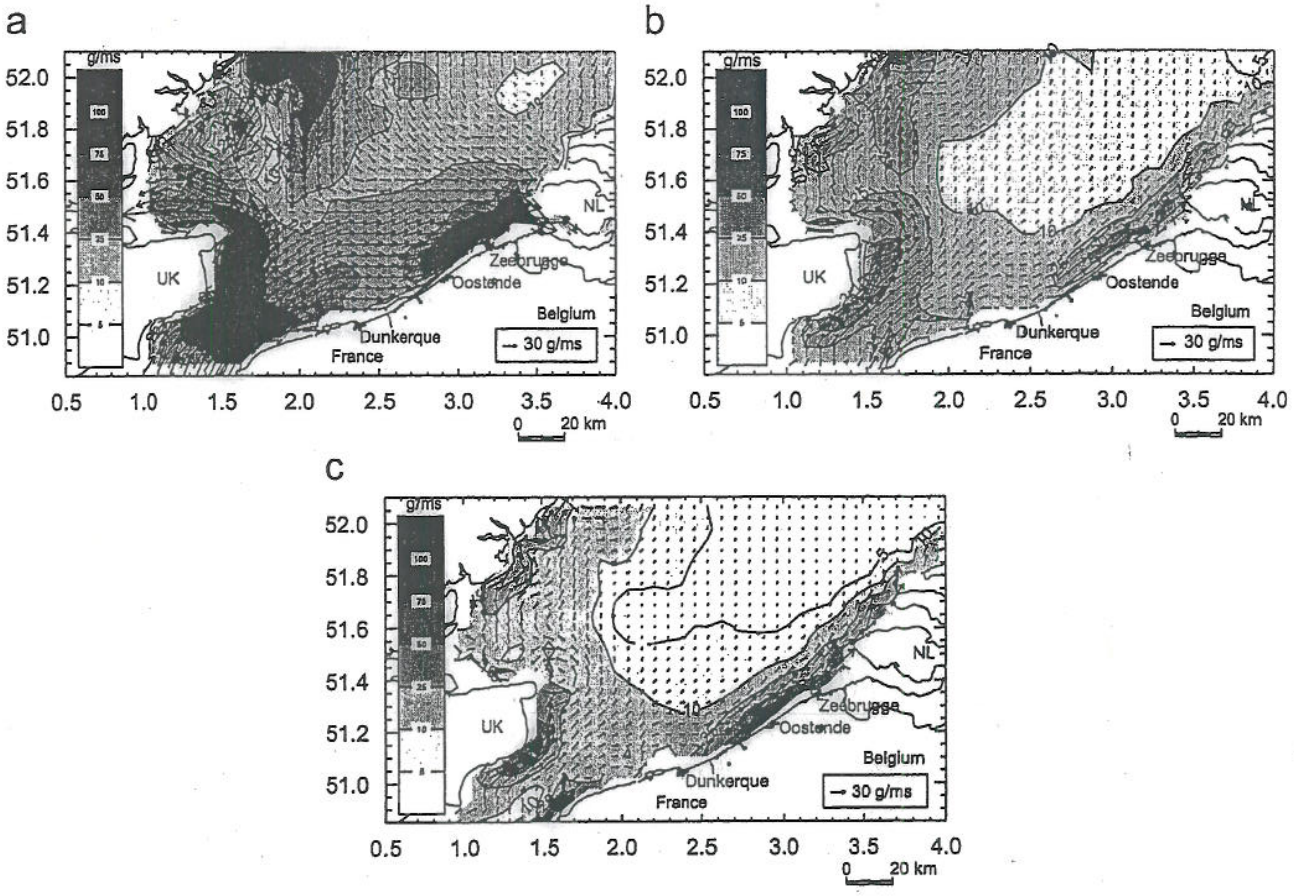

Fig. 8. Yearly averaged SPM transport per unit width (g/ms) in the southern North Sea, the x- and y-coordinates are in longitude (°E) and latitude (°N), respectively. The SPM transport has been calculated using: (a) Eq. (1) and only 362 velocity and SPM concentration fields (method 1); (b) Eq. (1) and the velocity fields at every time step of the model with the interpolated SPM fields (method 2); and (c) Eq. (2). (method 3). The SPM concentration from the satellite pictures has been corrected vertically to obtain depth-averaged values.

Table 3
Residual SPM transport (10^6 ton/season or year) through the Dover Strait and through a cross section at 51.9°N for the period January 1997—December 2003 (positive is towards the north) for methods 2 and 3

		Spring	Summer	Autumn	Winter	Year
Method 2	Dover Strait	3.36	2.50	9.18	7.22	22.26
	51.9°N	7.32	7.83	23.55	21.87	60.57
	Dover Strait—51.9°N	−3.96	−5.33	−14.37	−14.65	−38.31
Method 3	Dover Strait	3.00	4.19	14.02	10.53	31.74
	51.9°N	6.30	4.45	14.80	15.57	41.12
	Dover Strait—51.9°N	−3.00	−0.26	−0.78	−5.04	−9.08

The SPM concentrations have been vertically corrected to obtain depth averaged concentrations. 'Dover Strait—51.9°N' is the difference between inflow and outflow at both section, positive means a higher SPM flux into the southern North Sea than out of it.

i.e. the accuracy of SPM concentration in a cross section. This is due to the fact that (1) not enough long term SPM concentration measurements are available to correct the satellite images and to derive the long term residual SPM transport and (2) SPM concentration varies as a function of tide, wind, spring-neap tidal cycles and—because winds (storm surges) are not equally distributed during a year—also depends on the seasonal time scale (Jones et al., 1994; Fettweis et al., 2005, 2006). The short term

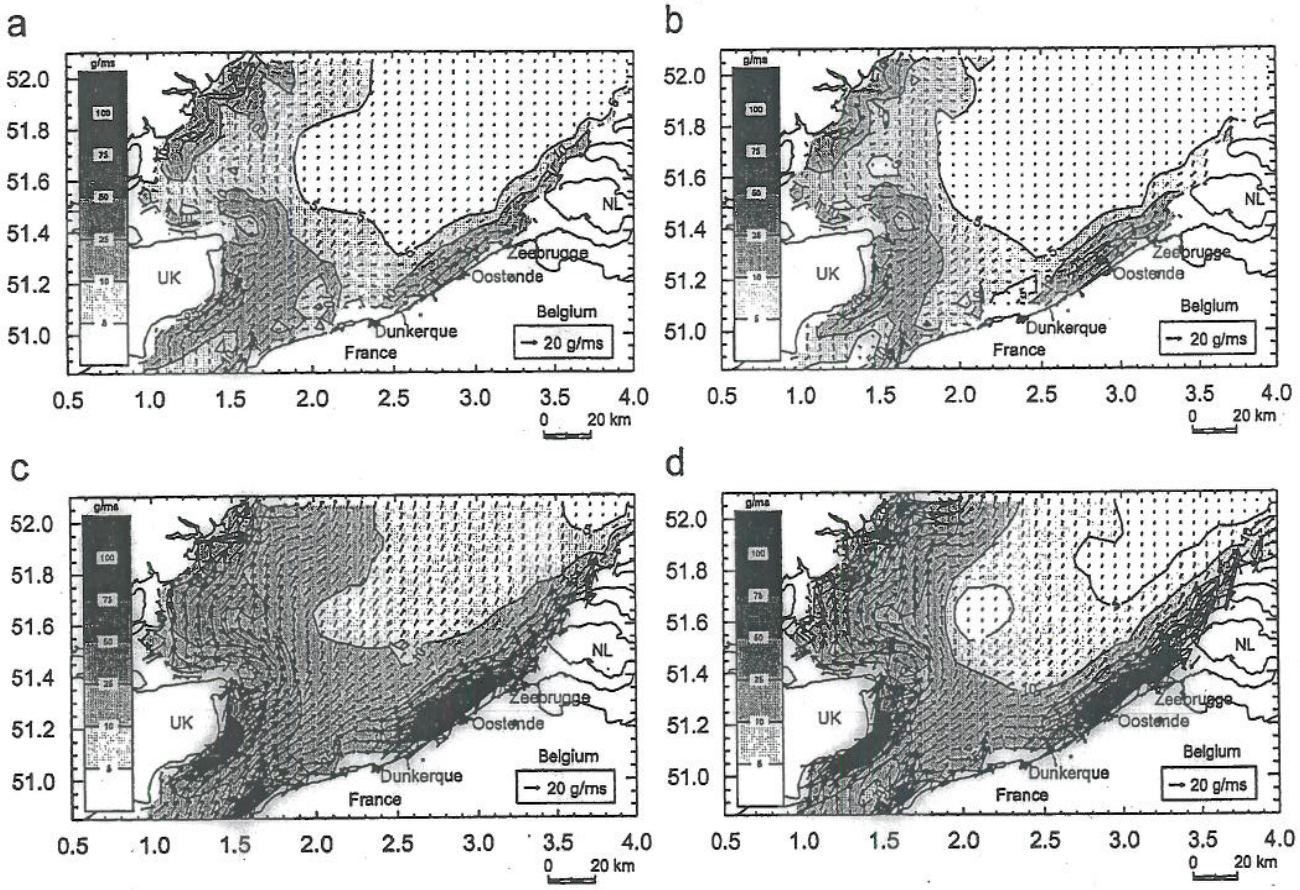

Fig. 9. Seasonal averaged SPM transport per unit width (g/ms) in the southern North Sea, the x- and y-coordinates are in longitude (°E) and latitude (°N), respectively. The SPM transport has been calculated using method 3 (Eq. (2)). The SPM concentration from the satellite pictures has been corrected vertically to obtain depth averaged values: (a) spring; (b) summer; (c) autumn; and (d) winter situation.

variations (tidal, spring-neap tidal cycle) have not been found back in the satellite images, however seasonal variations are clearly visible (Figs. 4 and 5). The satellite images have been taken during cloud-free conditions and low mean wind speeds (about 3.7 m/s) and are correlated with good weather conditions; increased SPM concentration due to higher wave erosion is seldom to be expected in these images.

The representativness of SPM concentration maps derived from satellites for calculating long term averaged transports has been investigated by comparing the SPM concentration variability from in situ measurements with those of remote sensing data. In Fig. 10 the relative variability in the in situ measurements and in the satellite data is shown as a function of the seasonally averaged SPM concentration. The figure (Fig. 10a) shows that the relative variability in the tidal cycle measurements (standard deviation of SPM concentration during a tidal cycle divided by tidally averaged SPM concentration) increases with increasing SPM concentration. This means that in the coastal turbidity maximum zone the SPM concentration variations are high during a tidal cycle, whereas outside or at the edge of the turbidity maximum, where the SPM concentrations are low, the tidal variability is also low. The 'snapshot' SPM concentration measured in MUMM's monitoring stations (Fig. 10b) is generally lower and the variability higher when compared with the tidal cycle measurements. Fig. 10c shows the variability in the pixels of the satellite images situated in the Belgian coastal area as a function of the seasonally averaged SPM concentration The figure indicates that (1) the SPM concentrations are generally lower from satellite data than from in situ tidal cycle measurements, (2) the relative variability decreases for lower and higher SPM concentrations and has a maximum at about 20 mg/l during spring and summer and at about 40 mg/l during autumn

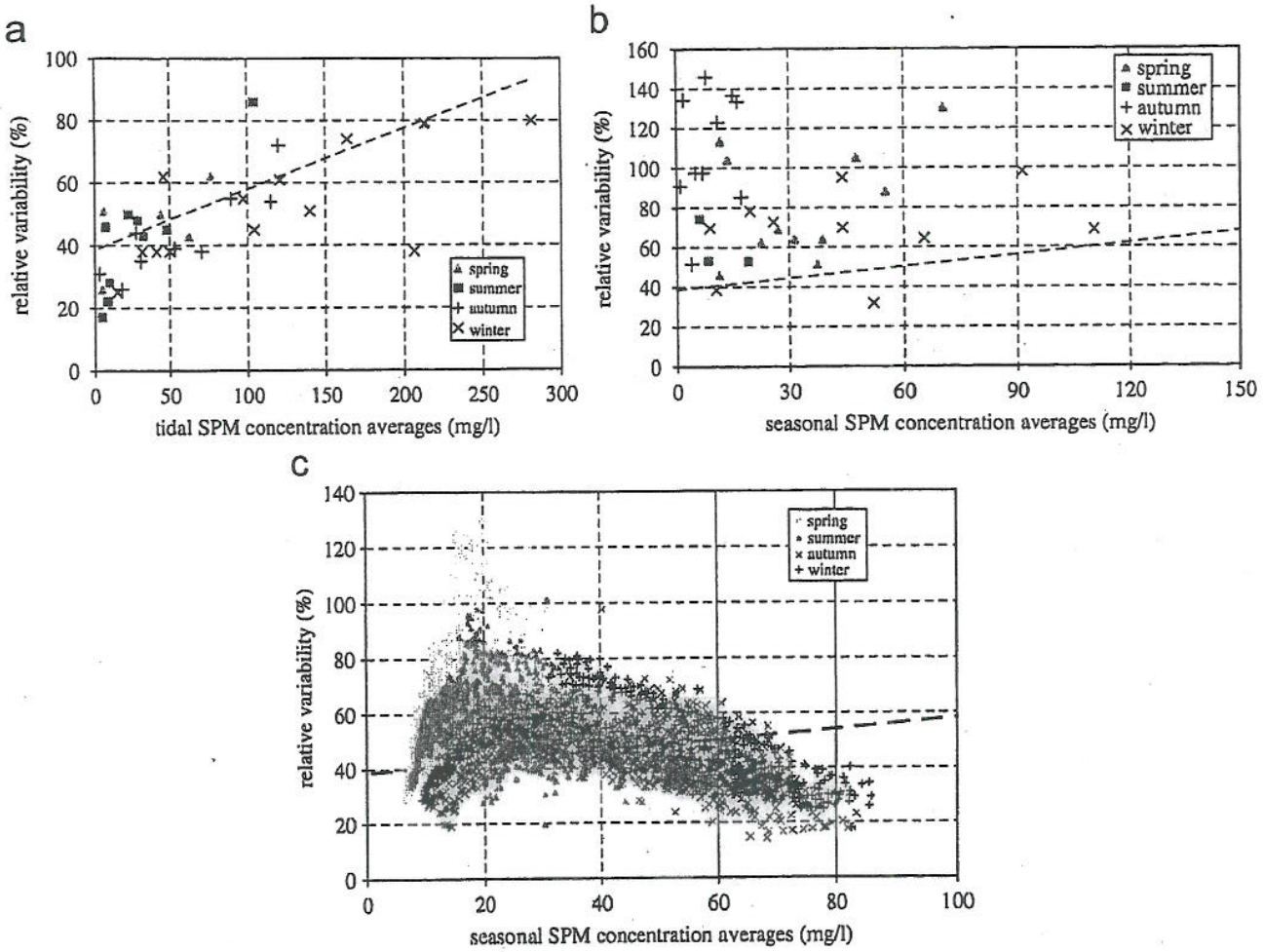

Fig. 10. (a) Relative variability in the tidal cycle stations during the period 1999–2005 as a function of tidal averages of SPM concentration. The samples have been taken at about 3 m from the bottom. (b) Relative variability in MUMM's monitoring stations during the period 1987–2004 as a function of seasonal averaged SPM concentration. Only stations with at least 10 samples have been selected. The samples have been taken at 3 m below the surface. (c) Relative variability in the pixels of the 362 SeaWiFS surface SPM concentration maps (1997–2004) situated in the Belgian–Dutch coastal zone (51.1°N–51.5°N and 2.7°E–3.5°E) as a function of seasonal averaged SPM concentration. The trendline in (b) and (c) is from in situ tidal measurements.

and winter, (3) the relative variability is of the same order of magnitude in most pixels as in the in situ tidal measurements (20–80%) except during spring and summer when relative variability's of up to 140% have been calculated and (4) that the very high variability at low concentrations is also found back in the in situ 'snapshot' measurements from MUMM's monitoring stations.

The maximum SPM concentration extracted from the satellite images is about 75–100 mg/l (surface) and 150–200 mg/l (depth averaged correction), whereas the maximum from the in situ 'snapshot' measurements is 680 mg/l (3 m below surface) and from the tidal cycle measurements nearly 1000 mg/l (3 m above bottom). Satellite images and the in situ measurements from MUMM's monitoring stations are both snapshots of the SPM concentration during a tidal cycle and have been sampled at the surface or near the surface (3 m below). The decreasing variability in satellite images and in the 'snapshot' in situ measurements with increasing SPM concentration could be explained if most of the SPM in the Belgian coastal zone during a tidal cycle would occur in the bottom layer of the water column and would thus be invisible for satellites or near surface sampling. Tidal measurements however indicate that strong vertical gradients and high SPM concentrations only occur during about 1/3 of the tidal cycle (2 h per ebb and flood) and that during the rest of

the cycle the measured SPM stratification and concentration is much lower (Van den Eynde et al., 2006). The low variability at higher concentration is therefore probably an artefact of the fact that the algorithm for processing the satellite images is underestimating the SPM concentration at higher values. The very high variability at low concentrations could thus be due to short-lived events, such as storms or high river runoff, which may increases locally the SPM concentration significantly and which may move the turbidity maximum zone more towards the coast or more offshore, as found in the salinity variations in the coastal area (Lacroix et al., 2004). During winter and autumn, the SPM concentration is already high and these events are therefore statistically less significant.

The relative variability of SPM concentration in the southern North Sea derived from satellite images is presented in Fig. 11. The SPM variability in the southern North Sea generally increases from the coast towards offshore and then decreases until about the central part of the southern North Sea, where a minimum is reached. The high relative variability band along but off the coast reflects the edge of the coastal turbidity maximum, which is not constant. In the Belgian–Dutch coastal waters the SPM concentration remains high during all the year; the extension of the coastal turbidity maximum is however changing with the seasons, it is furthest off shore during winter and nearest during summer.

Measurements in the Dover Strait, where the SPM concentration is generally low (<10 mg/l), have indicated that the vertical gradient is negligible most of the time (Van Alphen, 1990). The tidal cycle measurements in the Belgian coastal zone show that the vertical SPM concentration variation is low in low SPM concentration areas, therefore satellite images may give a good estimate of the total SPM concentration. In areas with higher turbidity the vertical variation during a tidal cycle is important and corrections have to be applied to obtain depth averaged values.

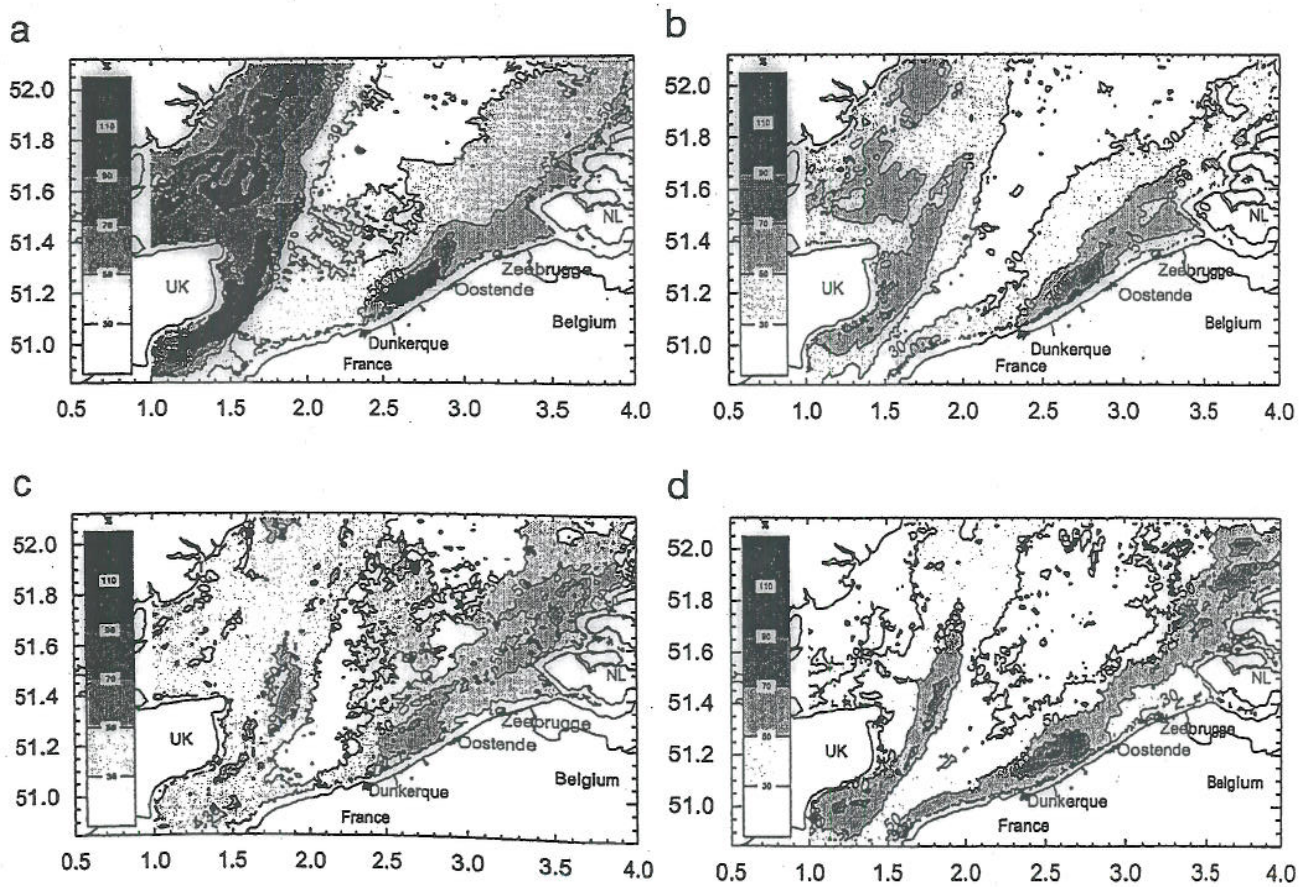

Fig. 11. Relative variability of the seasonal surface SPM concentration maps derived from 362 satellite images (see Fig. 4), the x- and y-coordinates are in longitude (°E) and latitude (°N). (a) spring, (b) summer, (c) autumn and (d) winter situation.

5. Conclusions

Three methods have been presented where satellite images, in situ measurements and hydrodynamic model results have been combined to calculate the long term SPM flux in the southern North Sea. The results indicate a flux through the Dover Strait of 22.26×10^6 or 31.74×10^6 t/yr; both fluxes have been calculated using the vertically corrected SPM concentrations. The latter SPM flux, which is calculated by multiplying the seasonally residual discharge with the seasonally averaged SPM concentration, is believed to be the most accurate one with the given data, because the inflow of SPM through the Dover Strait towards the North Sea is better conserved in the outflow through a section at 51.9°N.

The too low value of SPM concentration in the satellite imagery can be explained by:

(1) The fact that the procedure for processing the satellite images has been set up and validated for SPM concentration between 10 and 80 mg/l. For extremely turbid (SPM concentration >80 mg/l) and clear waters (SPM concentration <10 mg/l) the algorithm has not been validated and gives probably less accurate results (Nechad et al., 2003).
(2) Most satellite pictures are acquired in good weather conditions, whereas in situ measurements from a vessel can be carried out also during rougher meteorological conditions. In order to include all weather condition, long term measurements from stand alone frames have to be carried out.
(3) Due to the too low time resolution of the satellite images and snapshot in situ measurements, peaks of SPM concentration are often missed. It is therefore important to measure during at least one tidal cycle in the high turbidity area to obtain representative values of SPM concentration.

Satellite images are a major source of SPM concentration data and are the only way to obtain a spatial distribution for large areas, but they underestimate the SPM concentration. In order to calculate more accurately the total sediment flux further in situ measurements and/or numerical model results are needed to obtain vertical profiles of SPM concentration and to improve the algorithm for processing and correcting the satellite images.

Acknowledgements

This study was partly funded by the Maritime Access Division of the Ministry of the Flemish Community in the framework of the MOMO project and partly by the Belgian Science Policy within the framework of the MOCHA, BELCOLOUR and MAREBASSE projects. The measurements have been collected onboard of the R/V Belgica and R/V Zeeleeuw. The support of the measuring service of MUMM is acknowledged. The receiving station of Dundee University, Orbimage, the SeaWiFS and SeaDAS project teams, and the Distributed Active Archive Centre at GSFC are acknowledged for providing, distributing and supporting SeaWiFS data. We wish to acknowledge Virginie Pison (MUMM) who has greatly improved the paper during the many discussions and helpful suggestions. Fritz Francken (MUMM) is acknowledged for his help in compiling the measurement data.

Appendix A. Bio-optical model to derive SPM concentration

A.1. Method

The objective is to express SPM concentration in terms of the water-leaving reflectance. In the red and near infra red (NIR) spectral range, backscattering from pure water, coloured dissolved matter and yellow substance are negligible compared to the high backscattering of suspended sediments, hence SPM concentration, denoted by c, is linearly related to the backscattering $b_b(\lambda)$, at a given wavelength, λ in the red and NIR by:

$$b_b = c b_{bs}^*, \tag{A.1}$$

where b_{bs}^* is the specific backscatter coefficient (the λ-symbol is dropped for brevity). The reflectance just below the water surface, R_-, is function of the backscattering b_b and absorption a of light in the water (Gordon et al., 1998):

$$R_- = Q\left[l_1 \frac{b_b}{a+b_b} + l_2\left(\frac{b_b}{a+b_b}\right)^2\right]. \tag{A.2}$$

The coefficients $l_1 = 0.095$ and $l_2 = 0.079$ are derived from radiative transfer simulations and Q-factor is the ratio of the upwelling radiance in the viewing direction to the upwelling irradiance. The subsurface irradiance reflectance is related to

the water-leaving reflectance by the relationship (Mobley, 1994):

$$\rho_w = \pi \frac{t_{w\to a} t_{a\to w}}{Q n_w^2} \frac{R_-}{1 - rR_-}, \quad (A.3)$$

where $t_{w\to a}$ is the bidirectional radiance transmittance from water to air, $t_{a\to w}$ the irradiance transmittance from air to water; typical values for these factors, for the sun at the zenith are: $t_{w\to a} = 0.98$, $t_{a\to w} = 0.96$. $n_w = 1.34$ is the real part of the refractive index of water and $r = 0.48$ is the water–air reflectance for totally diffuse irradiance. Therefore Eq. (A.3) becomes

$$\rho_w = \pi \frac{0.52}{Q} \frac{R_-}{1 - rR_-}. \quad (A.4)$$

Eqs. (A.1), (A.2) and (A.4) are combined to give

$$c = \alpha \frac{\rho_w}{\gamma - \rho_w} \quad (A.5)$$

with $\alpha = a/(b_{bs}^*(1 - rQl_1))$ and $\gamma = 0.52\pi l_1/(1 - rQl_1)$. Replacing Q by the average value $Q = 3.7$sr for turbid waters (Gons, 1999) gives $\gamma = 0.187$.

A.2. Data sets

Measurements of water-leaving reflectance ρ_w were carried out from 2001 to 2003 using a system of three Trios spectro-radiometers with 2.5 nm resolution covering the spectral bandwidth [350–950 nm] and following the protocol described by Park et al. (2003). SPM concentrations were recorded at the same locations with a GF/F filter using the gravimetric method (see Section 2.3), for water samples taken between 0.5 and 3 m depth.

Amongst the collected measurements, 41 data sets of $\rho_w{}^\lambda$ and SPM concentrations were selected on the basis of the similarity spectrum criteria (Ruddick et al., 2006) and were convoluted with the SeaWiFS response function. Nonlinear regression analysis was applied to each band i with the following equation:

$$c = \beta^i + \frac{\alpha^i \rho_w^i}{0.187 - \rho_w^i}, \quad (A.6)$$

where α^i and β^i are the parameters to be calibrated for each band; β^i accounts for SPM concentration and reflectance measurement errors. The best curve fitting data with Eq. (A.6) was found for band 670 nm, which is given by Eq. (3).

References

Bailly du Bois, P., Salomon, J.C., Gandon, R., Guéguéniat, P., 1995. A quantitative estimate of English Channel water fluxes into the North Sea from 1987 to 1992 based on radiotracer distribution. Journal of Marine Systems 6, 457–481.

Bastin, A., 1974. Regionale sedimentologie en morfologie van de zuidelijke Noordzee en het Schelde estuarium. Katholieke Universiteit Leuven, pp. 91.

de Haas, H., 1997. Transport, preservation and accumulation of organic carbon in the North Sea, Ph.D. Thesis, Utrecht University, The Netherlands, pp. 149.

Dyer, K.R., Moffat, T.J., 1998. Fluxes of suspended matter in the East Anglian plume, southern North Sea. Continental Shelf Research 18, 1311–1331.

Eisma, D., 1981. Supply and deposition of suspended matter in the North Sea. In: Nio, D.D., Shuttenhelm, R.T.E., van Weering, T.C.E. (Eds.), Holocene Marine Sedimentation in the North Sea Basin. International Association of Sedimentolgy, Special Publication 5. Blackwell Scientific Publication, Oxford, pp. 415–428.

Eisma, D., Irion, G., 1988. Suspended matter and sediment transport. In: Salomons, W., Bayne, W.L., Duursma, E.K., Förstner, U. (Eds.), Pollution of the North Sea: An Assessment. Springer, Berlin, pp. 20–35.

Fettweis, M., Van den Eynde, D., 2003. The mud deposits and the high turbidity in the Belgian–Dutch coastal zone, southern bight of the North Sea. Continental Shelf Research 23, 669–691.

Fettweis, M., Francken, F., Van den Eynde, D., Houziaux, J.-S., Vandenbergh, N., Fontaine, K., Deleu, S., Van Lancker, V., Van Rooij, D., 2005. Mud origin, characterisation and human activities (MOCHA): characteristics of cohesive sediments on the Belgian Continental Shelf. Scientific Report Year 1. Belgian Science Policy, Brussel, pp. 70.

Fettweis, M., Francken, F., Pison, V., Van den Eynde, D., 2006. Suspended particulate matter dynamics and aggregate sizes in a high turbidity area. Marine Geology 235, 63–74.

Garreau, P. (Eds.), 1997. Task N: numerical hydrodynamic modelling. In: Hydrodynamics Biogeochemical Processes and Fluxes in the Channel, FLUXMANCHE II Final Report, MAS2CT940089. pp. 12–38.

Gerritsen, H., Boon, J.G., van der Kaaij, T., Vos, R.J., 2001. Integrated modelling of suspended matter in the North Sea. Estuarine, Coastal and Shelf Science 53, 581–594.

Gons, H.J., 1999. Optical teledetection of chlorophyll a in turbid inland waters. Environmental Science and Technology 33, 1127–1132.

Gordon, H.R., Brown, O.B., Evans, R.H., Brown, J.W., Smith, R.C., Baker, K.S., Clark, D.K., 1998. A semianalytic radiance model of ocean color. Journal of Geophysical Research 93, 10909–10924.

Jones, S.E., Jago, C.F., Prandle, D., Flatt, D., 1994. Suspended sediment dynamics: measurements and modelling in the dover strait. In: Beven, K.J., Chatwin, P.C., Milbank, J.H. (Eds.), Mixing and Transport in the Environment. Wiley, pp. 183–201.

Lacroix, G., Ruddick, K., Ozer, J., Lancelot, C., 2004. Modelling the impact of the Scheldt and Rhine/Meuse plumes on the salinity distribution in Belgian waters (southern North Sea). Journal of Sea Research 52 (3), 149–163.

Lafite, R., Shimwell, S.J., Nash, L.A., Dupont, J.P., Huault, M.F., Grochowski, N.T.L., Lamboy, J.M., Collins, M.B., 1993. Sub-Task S1: suspended material fluxes through the Strait of Dover, hydrodynamics and biogeochemical fluxes in the Eastern Channel: fluxes into the North Sea. FLUXMANCHE I Second Annual Report, MAST 0053-C (EDB), pp. 81–106.

Luyten, P.J., Jones, J.E., Proctor, R., Tabor, A., Tett, P., Wild-Allen, K., 1999. COHERENS a coupled hydrodynamical-ecological model for regional and shelf seas: user documentation. MUMM Report, Brussels. pp. 911. [Available on CD-ROM at ⟨http://www.mumm.ac.be/coherens⟩].

McManus, J.P., Prandle, D., 1997. Development of a model to reproduce observed suspended sediment distributions in the southern North Sea using principal component analysis and multiple linear regression. Continental Shelf Research 17, 761–778.

Mikkelsen, O.A., Pejrup, M., 2001. The use of a LISST-100 laser particle sizer for in situ estimates of floc size, density and settling velocity. Geo-Marine Letters 20, 187–195.

Mobley, C.D., 1994. Applied Electromagnetics and Optics Laboratory—SRI Int. Light and Water—Radiative Transfer in Natural Waters. Academic press, Inc.

Nechad, B., De Cauwer, V., Park, Y., Ruddick, K., 2003. Suspended particulate matter (SPM) mapping from MERIS imagery. Calibration of a regional algorithm for the Belgian coastal waters. Proceedings MERIS User Workshop, 10–13th November 2003, Frascati. European Space Agency Special Publication SP-549, ESA Publication Division, Noordwijk, The Netherlands, pp. 6. ⟨http://www.mumm.ac.be/BELCOLOUR/Publications/MERISUsers2003BNwithheader.pdf⟩.

Park, Y., De Cauwer, V., Nechad, B., Ruddick, K., 2003. Validation of MERIS water products for Belgian coastal waters: 2002–2003. MERIS and AATSR Calibration and Geophysical Validation workshop, 20–24th October 2003 (Frascati). European Space Agency WPP-223. ⟨http://www.mumm.ac.be/BELCOLOUR/Publications/MUMM-MAVT2003.pdf⟩.

Prandle, D., 1993. Year-long measurements of flow through the Dover Strait by H.F. Radar and acoustic Doppler current profiler (ADCP). Oceanologica Acta 16 (5–6), 457–468.

Prandle, D., Loch, S.G., Player, R., 1993. Tidal flow through the Dover Strait. Journal of Physical Oceanography 23, 23–37.

Prandle, D., Ballard, G., Flatt, D., Harrison, A.J., Jones, S.E., Knight, P.J., Loch, S.G., McManus, J.P., Player, R., Tappin, A., 1996. Combining modelling and monitoring to determine fluxes of water, dissolved and particulate metals through the Dover Strait. Continental Shelf Research 16 (2), 237–257.

Ruddick, K., Ovidio, F., Rijkeboer, M., 2000. Atmospheric correction of SeaWiFS imagery for turbid coastal and inland waters. Applied Optics 39 (6), 897–912 ⟨http://www.mumm.ac.be/OceanColour/Publications/ATCOR2000AO.pdf⟩.

Ruddick, K., De Cauwer, V., Park, Y., Moore, G., 2006. Seaborne measurements of near infrared water-leaving reflectance: the similarity spectrum for turbid waters. Limnology and Oceanography 51, 1167–1179 ⟨http://aslo.org/lo/toc/vol_51/issue_2/1167.pdf⟩.

Salomon, J.C., Breton, M., Guegueniat, P., 1993. Computed residual flow through the Dover Strait. Oceanologica Acta 16 (5–6), 449–455.

Van Alphen, J.S.L.J., 1990. A mud balance for Belgian–Dutch coastal waters between 1969 and 1986. Netherlands Journal of Sea Research 25, 19–30.

Van den Eynde, D., Nechad, B., Fettweis, M., Francken, F., 2006. SPM dynamics in the southern North Sea derived from SeaWifs imagery, in situ measurements and numerical modelling. In: Maa, J.P.-Y., Sanford, L.P., Schoelhammer, D.H. (Eds.), Estuarine and Coastal Fine Sediment Dynamics. Proceedings in Marine Science, vol. 8. Elsevier, Amsterdam.

van Leussen, W., 1994. Estuarine macroflocs and their role in fine-grained sediment transport. University Utrecht, Utrecht, pp. 488.

Velegrakis, A.F., Bishop, C., Lafite, R., Oikonomou, E.K., Lecouturier, M., Collins, M.B., 1997. Sub-Task S3: Investigation of meso- and macro-scale sediment transport, hydrodynamics biogeochemical processes and fluxes in the channel. FLUXMANCHE II Final Report, MAST II, MAS2CT940089, pp. 128–143.

Winterwerp, J., 1998. A simple model for turbulence induced flocculation of cohesive sediments. Journal of Hydraulic Research 36 (3), 309–326.